Monte Carlo simulations for the evaluation of various influence factors on projections in computed tomography

B. Chyba and M. Mantler[a)]
Technische Universität Wien, Vienna, Austria

M. Reiter
Fachhochschule Wels, Wels, Austria

(Received 23 March 2010; accepted 25 March 2010)

This paper presents Monte Carlo simulations considering all stages of the creation process of two-dimensional projections in a computed tomography (CT) device: excitation of angle dependent X-ray spectra within the X-ray tube using results from a previous study [Chyba *et al.* (2008). Powder Diffr. **23**, 150–153]; interaction of these X-rays and secondary photoelectrons with a simple inhomogeneous sample; and interaction of X-rays and photoelectrons with the components (thin layers) of a matrix scintillation detector. The simulations were carried out by using custom software running on up to 50 nodes of a computer cluster. Comparative calculations were also made by using the software package MCNP [Booth *et al.* (2003). MCNP—A general Monte Carlo *N*-particle transport code, Report LAUR 03-1987, Los Alamos National Laboratory, Los Alamos, NM]. Tube spectra were calculated with algorithms proposed by Ebel [(2006). Adv. X-Ray Anal. **49**, 267–273]. Measurements for the chosen setup made with an available CT device were in relatively good agreement with calculated results. It was shown that good knowledge of the tube spectra is of importance, but most differences between resulting projections and measurements are caused by uncertainties concerning detector response due to light yield of the scintillator and to internal scattering effects within the thin detector layers which lead to spreading of a detected point signal within the detector matrix into neighboring matrix elements. © *2010 International Centre for Diffraction Data.* [DOI: 10.1154/1.3394014]

Key words: computed tomography, Monte Carlo simulation, detector modeling

I. INTRODUCTION

Computed tomography (CT) has become a widely used technique for nondestructive material testing in industry. A common setup of a CT device consists of an X-ray tube utilizing a cone beam and a matrix scintillation detector for recording two-dimensional (2D) projections. A set of projections is used to reconstruct a three-dimensional (3D) image for visualization of the sample. Aside from the advantage of image magnification, CT in cone beam geometry leads to difficulties in the quality of the back-calculated image due to the complex mathematical reconstruction process. It is therefore highly sensitive to artifacts caused by sometimes unaccounted physical interactions of X-rays with the sample and X-rays with the detector components, such as elastic and inelastic scatterings of radiation with the specimen, scatterings in air, and scatterings in the layers of the detector, as well as the details of the angular dependent spectral distribution of the X-ray beam and the general complexity of the energy dependence of interactions.

Many adverse influences can be minimized by optimization of experimental parameters (e.g., X-ray tube voltage, absorber plates, etc.). Experimental tests as a tool for the determination of an optimized setup of parameters for each measurement can however be very time consuming. An alternative is the computed simulation. We present a study of the complete process of formation of radiographic projections by using Monte Carlo (MC) techniques, aiming at a better understanding of the role of the various influence factors and thereby advancing the optimization of measurement parameters and the improvement of correction algorithms for the back calculation.

II. INSTRUMENTATION

Experiments have been carried out by using an industrial 3D CT system (Hans Wälischmiller Gmbh, Germany, model RayScan200) at the Upper Austrian University of Applied Sciences, Wels. A schematic diagram of the setup is shown in Figure 1. An illustration of the sample is shown in Figure 2.

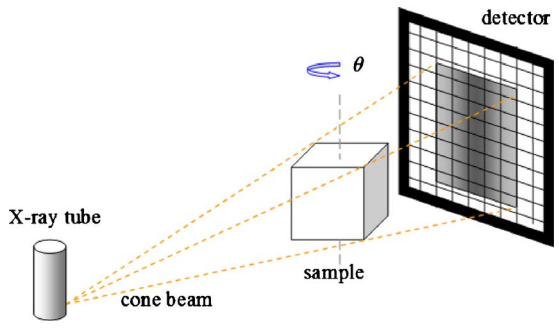

Figure 1. (Color online) Schematic diagram of the experimental setup and simulation illustrating the radiographic projection of the sample (Figure 2) by an X-ray cone beam onto a flat panel detector.

[a)]Author to whom correspondence should be addressed. Also at Vienna University of Technology, Wiedner Hauptstrasse 8-10/138 A, 1040 Vienna, Austria. Electronic mail: michael.mantler@ifp.tuwien.ac.at

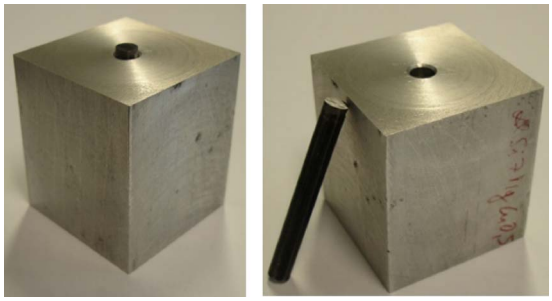

Figure 2. (Color online) Illustration of the sample used in all projection experiments and simulations in this paper; an aluminum cube of 4 cm edge length with a central cylindric opening (0.6 cm) which could be filled by a steal pole.

The setup is described elsewhere (Chyba *et al.*, 2008) in more detail. For the investigations in this paper the microfocus tube (Viscom 225 kV; 5 μm microfocus; W target) was used; an amorphous silicon matrix detector with a scintillating layer (Perkin Elmer RID 1640; 1024×1024 pixel, 410 mm×410 mm) is located at a fixed distance of 1540 mm. In between them, at a selectable distance, the sample object is positioned on a rotational stage.

III. SIMULATIONS

An existing software package (Ebel, 2006; Chyba *et al.*, 2008), originally developed to simulate the emitted angle dependent X-ray tube radiation and its interactions with a simple inhomogeneous sample (an aluminum cube with a cylindrical hole filled by air or steel shown in Figure 2), was upgraded to account also for interactions with the detector layers and determine the resulting energy deposited by radiation in the scintillator layer in order to provide for the detector response and spreading of the signal from each detector pixel to its neighboring pixels. All known interactions of X-rays with matter were considered as far as they give measurable contributions, including excitation of fluorescent radiation, coherent and incoherent scatterings, multiple combinations of these interactions, and secondary effects (secondary electrons, fluorescence, and bremsstrahlung) by photoelectrons and Auger electrons. The calculations were run on up to 50 nodes of a computer cluster located at the Vienna University of Technology. The software package has not yet been decided for being published.

Additional simulations for calculations of the detector efficiency and point spread functions (PSFs) were carried out with MCNP (Booth *et al.*, 2003) using a simple layer model: 500 μm graphite (scintillator coating), 550 μm Gd (scintillator, assumed to be a pure element rather than the real material Gd_2O_2S:Tb to reduce computing time), 200 μm Si (photodetector), and 3 mm C (board). It was, however, not possible to verify these assumptions by reliable information from the manufacturer.

The use of pure Gd instead of the real composition of the scintillator material leads to an estimated error of up to 2.4%, which is shown in the plot of Figure 3. An analytical function fit of the simulated PSF was applied on a projection image using MATLAB.

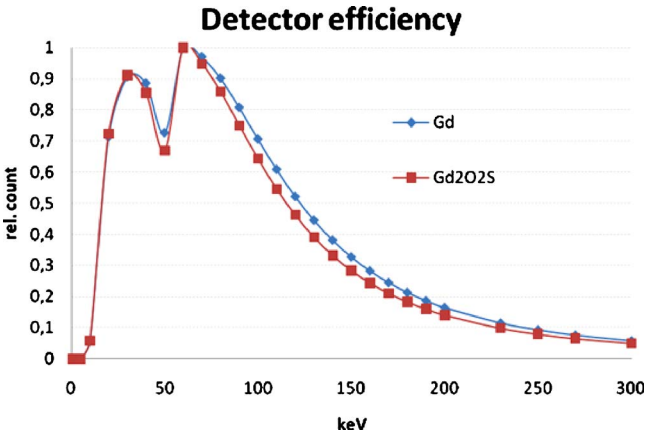

Figure 3. (Color online) Comparison of detector efficiency functions calculated analytically by using a simple layer model, assuming pure Gd (rhombs) and Gd_2O_2S (squares), as scintillator material.

IV. RESULTS

The detector efficiency was calculated by counting the energy deposited in the scintillation layer of the detector. A comparison of two calculation methods (an analytical model based mainly on the absorption of incident radiation by Gd and MC methods) with a measured efficiency function (Reitz *et al.*, 2007) is shown in Figure 4. The differences are quite significant. It has to be pointed out that the agreement of measurement and MC methods is better, but the number of comparable data points is small.

The energy deposited in the scintillator layer was also calculated as a function of the pixel index of the detector as shown in Figure 5. Additionally, scattering along the air path was taken into account in one of the plots. The simulation results were approximated by analytical fit functions to be used as a 2D filter for the projection simulations. These two PSFs were two-dimensionally convoluted with the projection image. Figure 6 shows the convolution with the lower PSF of Figure 5 (no air in beam). The differences to the nonfiltered

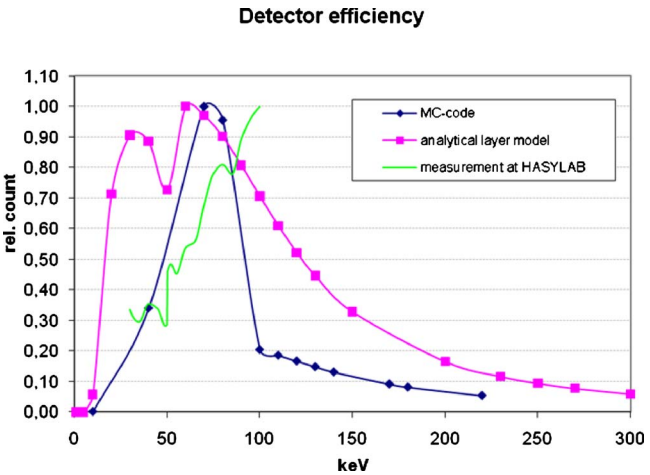

Figure 4. (Color online) Detector efficiency functions calculated analytically by using a simple layer model (squares) and Monte Carlo code (rhombs) both compared with a measured response function (line) of a similar detector model (Reitz *et al.*, 2007).

https://doi.org/10.1154/1.3394014 Published online by Cambridge University Press

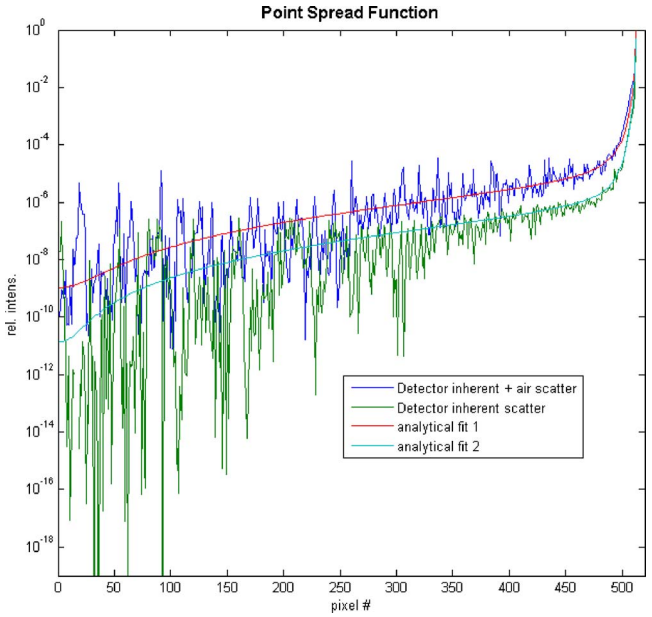

Figure 5. (Color online) Point spread function (half side) of a needle beam simulated at 200 keV for the assumed layer model of the detector. The plot shows the results accounting for detector inherent scatter only (lower plot) and its analytical fit function (lower smooth plot) and additionally accounting for air scatter (upper plot) and its analytical fit function (upper smooth plot).

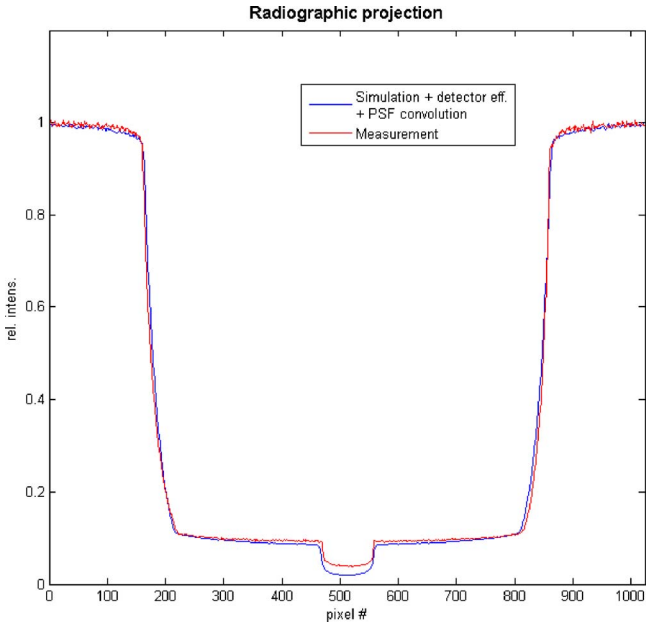

Figure 7. (Color online) Comparison of measured radiographic sample projection with simulated projection after convolution with PSF including air scatter and application of simulated detector response function. Despite the area behind the steel pole around pixel 512, the agreement of the simulated (lower plot) and the measured plot (upper plot) is very good.

image are small, which can be interpreted as a small and almost negligible influence of detector inherent scattering on image blurring in this setup.

In Figure 7 the convolution of the PSF including scattering in air was applied to the projection image as well as the previously shown detector efficiency calculated with MC code (Figure 4). Very good agreement could be achieved except for the region directly behind the steel pole where, due to beam hardening, the rate of high energy photons may be higher than simulated.

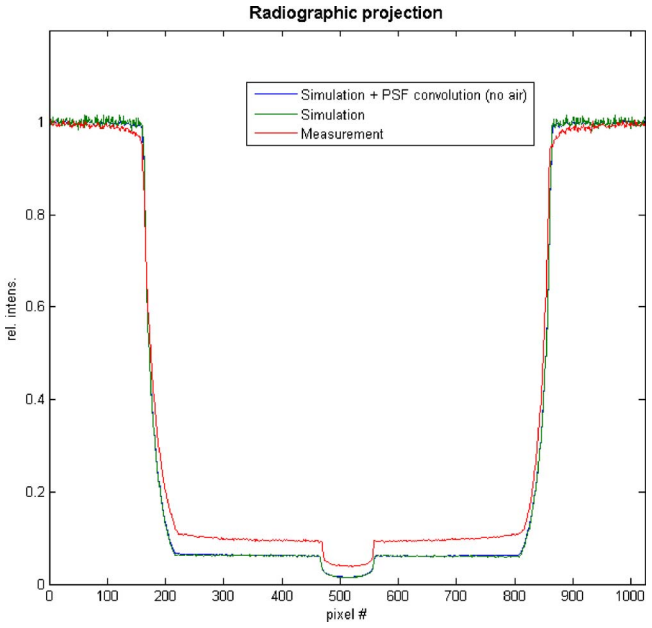

Figure 6. (Color online) Comparison of measured radiographic sample projection (upper plot) with simulated projection, and simulated projection after convolution with PSF not accounting for air scatter (lower plots). The lower plots are almost not distinguishable, which can be interpreted as negligible impact on image blurring by detector inherent scattering.

V. CONCLUSION

The simulated radiographic projection of an inhomogeneous specimen was filtered by a separately calculated point spread function and applied to a detector efficiency function which was also calculated in advance. Very good agreement could be achieved, though many simplifications had to be introduced.

The PSF was only calculated for 200 keV primary photons since PSFs of relevant lower primary energies were shaped similarly. The thicknesses of some layers in the detector model had to be estimated since no accurate data were provided by the manufacturer. The scintillator coating, for example, was only vaguely specified as either molybdenum or graphite which is not a negligible difference for the detector efficiency. The actual coating was found to be most likely graphite by comparison of simulated with experimental data. Hence the error of using pure Gd in the calculations, instead of the real scintillator composition, was of minor relevance.

The influence of the spectral distribution turned out to be of less importance since the detector efficiency function had a quite sharp maximum at about 70 keV. The influence of air is negligible when considering attenuation at energies of several 100 keV, but weak scattering of X-rays by air occurs

https://doi.org/10.1154/1.3394014 Published online by Cambridge University Press

along the relatively long distance (1.5 m) between tube and detector. This was accounted for in the PSF (detector inherent scattering with needle beam) rather than in the MC simulation of the radiographic projection.

ACKNOWLEDGMENT

This work was supported by the Österreichische Forschungsförderungsgesellschaft mbH, Project No. 812136-SCK/KUG.

Booth, T. E., Brown, F. B., Bull, J. S., Forster, R. A., Goorley, J. T., Hughes, H. G., Mosteller, R. D., Prael, R. E., Sood, A., Sweezy, J. E., Zukaitis, A., Marsha Boggs, M., and Roger Martz, R. (**2003**). MCNP—A general Monte Carlo *N*-particle transport code, Report LAUR 03-1987, Los Alamos National Laboratory, Los Alamos, NM.

Chyba, B., Mantler, M., and Reiter, M. (**2008**). "Monte-Carlo simulation of projections in computed tomography," Powder Diffr. **23**, 150–153.

Ebel, H. (**2006**). "Fundamental parameter programs: Algorithms for the description of K, L, and M spectra of X-ray tubes," Adv. X-Ray Anal. **49**, 267–273.

Reitz, I., Webb, M. A., Graafsma, H., Lohmann, M., Partridge, M., Tacke, M. B., Rau, A., Ulrich, S., Hesse, B.-M., Nill, S., and Oelfke, U. (**2007**). "Measurement of the radiation response of a flat-panel detector with monochromatic X-rays at HASYLAB," Radiother. Oncol. **84**, 79–80.